Eur. Phys. J. D **20**, 261–268 (2002)
DOI: 10.1140/epjd/e2002-00136-9

THE EUROPEAN PHYSICAL JOURNAL D

Photoexcitation of rare-gas neon and argon clusters doped with H_2O

A. Kanaev[1,a], L. Museur[2], F. Edery[1], T. Laarmann[3], and T. Möller[3]

[1] Laboratoire d'Ingénierie des Matériaux et des Hautes Pressions, CNRS, Institut Galilée, université Paris-Nord, 93430 Villetaneuse, France
[2] Laboratoire Physique des Lasers, CNRS, Institut Galilée, université Paris-Nord, 93430 Villetaneuse, France
[3] Hamburger Synchrotronstrahlungslabor HASYLAB at Deutsches Elektronen Synchrotron DESY, Hamburg, Notkestr. 85, 22603 Hamburg, Germany

Received 7 March 2002 / Received in final form 27 May 2002
Published online 19 July 2002 –

Abstract. We have studied the fluorescence of electronically excited OH^*, H^* and H_2O^{+*} dissociation fragments after VUV excitation ($h\nu \geq 11.6$ eV) of rare-gas clusters (Rg = Ne, Ar) doped with H_2O molecules. In contrast to a free molecule, where Balmer H-series dominate the UV-visible spectra, only the $OH^*(A^2\Sigma^+ \rightarrow X^2\Pi)$ emission band is observed in neon clusters. No emission of excited water ions has been observed. We find that while higher excitation energies (Ne *vs.* Ar) induce higher vibrational excitation of the $OH^*(A)$ fragment, the rotational temperature is lower. This effect is attributed to the difference in the geometric position of the H_2O molecule on the surface or inside the Rg-cluster. The rotational relaxation in neon clusters is rapid while the vibrational relaxation is slow because of the coupling with the low energy matrix phonons.

PACS. 36.40.Mr Spectroscopy and geometrical structure of clusters – 33.20.Lg Ultraviolet spectra – 33.20.Vq Vibration-rotation analysis

1 Introduction

The water molecule has been recognized as a very good model system for molecular dynamics studies in polyatomic systems. The photoexcitation of H_2O molecules in the vacuum ultraviolet region has been a subject of numerous publications [1–4]. Depending on the excitation energy, different excited states of OH^* and H^* dissociation fragments and of H_2O^{+*} can be produced. It has been found, that below the ionization limit situated at ∼12.6 eV, the H_2O molecule rapidly dissociates into the radical and the hydrogen atom in their ground states. Moreover, at excitation above 9.136 eV (135.71 nm) the electronically excited $OH^*(A^2\Sigma^+)$ fragment appears in the decay channel with a quantum yield below 10%. More decay channels open above the ionization limit.

The spectroscopy of free water molecules and the dissociation dynamics of some selected states in the VUV spectral energy range are rather well understood. It has been shown that the nsa_1 Rydberg states are repulsive in the bend configuration and undergo direct dissociation which results mainly in ground-state neutral fragments or ions. Other Rydberg states are bound but heavily predissociate (or/and preionize) *via* a repulsive potential. In particular, detailed analysis of the lowest bound $\tilde{C}^1B_1$ state shows its coupling with the $\tilde{B}^1A_1$ repulsive state, which has a sensitive dependence on the mean square momentum projection on the molecular axis a, $\langle J_a'^2 \rangle$ [5]. Much effort has also been paid to the spectroscopy of ejected excited $OH^*(A)$ fragments [6–8]. The rotational distribution has been found to be highly inverted with the maximum near the highest $J'_{\max}$-level energetically accessible at a given excitation energy. This $J'_{\max}$ value increases with the photon energy. The vibrational excitation of $OH^*(A)$ fragments is generally small. Matrix-isolated spectroscopy of H_2O molecules in rare-gas solids has also been applied for understanding the reaction dynamics in more detail. Series of studies have been devoted to the water photodissociation in the first absorption continuum at ∼7.5 eV, where the matrix cage effect has been observed [9–11].

Several studies on the reaction dynamics in a cluster environment have been performed (*e.g.* see issues [12]). In our work we are interesting in the spectroscopy of high-lying excited states of simple molecules embedded in clusters. In particularly, fluorescence spectra and the yield of excited products in clusters of different sizes reflect peculiarities of the reaction channels. Our recent experiments on doped cluster beams have shown the advantage of a fast sample renewal and the possibility of a detailed study of cluster size effects on the chemical reactivity and dynamics [13,14]. We are performing

[a] e-mail: kanaev@limhp.univ-paris13.fr

spectroscopic studies of rare-gas clusters doped with one H_2O molecule. As our first experiments have shown, He_N clusters ($N \approx 10^4$) have almost no influence on the photodissociation dynamics of embedded water molecules [15]. This is apparently related to the weak He–He and H_2O–He interactions and the high reaction energetics. On the other hand, the helium cluster atoms seem to effect the photoionization yield: the excited H_2O^{+*} ion channel is strongly suppressed inside the clusters. Since the binding energy of Rg-atoms in rare-gas solids increases in order of He(0.5 meV) → Ne(27 meV) → Ar(89 meV), one may expect that the cluster matrix effect increases in the same order. Therefore, we have carried out additional experiments with H_2O-doped neon and argon clusters. We discuss peculiarities of the energy relaxation process related to the cluster composition upon optical excitation in the VUV spectral region of 9–30 eV. These results complement our study of the cage-induced quenching of the excited photodissociation product OH(A), which will be published elsewhere [16].

2 Experiment

The measurements were performed at the experimental station CLULU at the synchrotron radiation laboratory HASYLAB in Hamburg [17]. Recent experiments on H_2O-doped helium clusters at CLULU were described in reference [15]. In present studies the rare-gas clusters were prepared in a continuous free-jet expansion of a pure gas through an orifice-type nozzle of 40 μm diameter or through a conical-shaped nozzle ($D = 200\,\mu$m, $2\theta = 4°$). The nozzle is mounted on a liquid He cryostat which can be cooled to temperatures below 10 K. The orifice-type nozzle was used to prepare Ar_N clusters and was operated at room temperature and a stagnation pressure of 80 bar ($N \approx 400$ atoms/cluster). To prepare Ne_N clusters a conical nozzle was used. At a temperature of 30 K with a stagnation pressure of 200 mbar, Ne_N clusters with an average size of approximately $N \approx 7\,500$ atoms/cluster were produced. The doped $H_2O@Rg_N$ clusters were prepared in a pick-up process of H_2O molecules from a cross-jet. The cross-jet intersects with the cluster beam 5 mm downstream from the cryogenic nozzle. The doped clusters were excited with synchrotron radiation (SR) and analyzed next to the intersection cross-point before their arrival at the Mach disk and disappearance by heating. Tunable SR ($\Delta\lambda = 0.05$ nm) in the spectral range of 100–140 nm (Al-grating) or 40–100 nm (Pt-grating) was focused on the doped cluster beam 10 mm downstream from the nozzle. Fluorescence excitation spectra (VUV–UV and visible–IR) were recorded by two suitable detectors containing CsI and GaAs(Cs) photocathodes. Energy-resolved fluorescence spectra in the UV and the visible were collected with a liquid nitrogen cooled CCD camera (Princeton Instruments) installed after a monochromator ($f = 275$ mm, 150 or 1 200 l/mm gratings, 250 or 80 μm slits). The background pressure was kept below 10^{-3} mbar during the experiments by continuous pumping of the interaction volume with a large (2 200 l/s) turbomolecular pump.

The mean cluster size N has been determined using well-known scaling laws [18–20]. The cluster size distribution in the nozzle expansion experiments has a width (FWHM) of $\Delta N \approx N$.

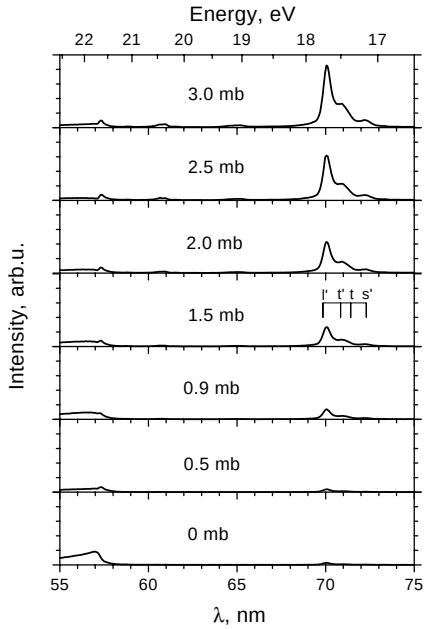

Fig. 1. UV-visible-IR fluorescence excitation spectra of $H_2O@Ne_N$ clusters ($N \approx 7\,500$ atoms/cluster). The H_2O-crossbeam stagnation pressures are indicated in the figure. Vertical lines indicate the $n = 1, 1'$ excitons of solid neon.

3 Results and discussion

3.1 $H_2O@Ne_N$-clusters

UV-visible-IR excitation spectra of $H_2O@Ne_{7500}$ clusters are shown in Figure 1. For comparison, an excitation spectrum of pure neon clusters in the same spectral region as well as a VUV excitation spectrum of the pure Ne clusters are presented in Figure 2. As it has been previously discussed in reference [21], the excitation of Ne_N clusters results in the broad VUV fluorescence continuum at ∼16.5 eV assigned to atomic (a-STE) and molecular (m-STE) centers inside the clusters. This is in general agreement with experiments in the solid neon [22]. Visible and IR bands are due to desorbed excited surface atoms [23]. The first excitonic band at ∼70 nm (labeled $n = 1$) contributes to the VUV continuum and the higher-n excitons – to the visible and IR spectra (see in Fig. 2). In agreement with these results, almost no fluorescence in the UV-visible-IR spectral range has been observed in Ne_N clusters upon excitation of the first excitonic absorption bands using a detector sensitive in that range. On the other hand, the 70-nm band in the UV-visible-IR excitation spectra linearly increases in intensity when the H_2O-cross-jet pressure grows (see Fig. 1).

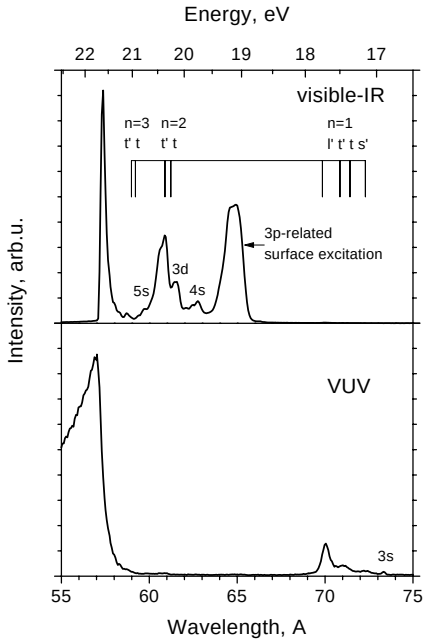

Fig. 2. VUV and visible-IR fluorescence excitation spectra of pure Ne_N clusters ($N \approx 7\,500$ atoms/cluster). Vertical lines indicate the excitons of solid neon and additionally some atomic excited Ne states are marked.

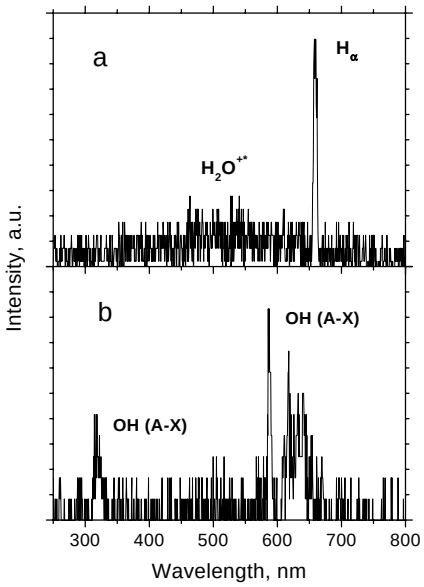

Fig. 3. Low-resolution fluorescence spectra of free water molecule (a) and that of $H_2O@Ne_N$ clusters (b) with excitation at 70.05 nm (identification of peaks is given in the high resolution spectrum presented in Fig. 4).

This is related to the energy transfer process from the cluster atoms to the water molecule, which dissociates, producing the excited $OH^*(A)$ fragment and which fluorescence at $\lambda_{\text{fluo}} \approx 315$ nm ($\tau \sim 800$ ns) is seen by the detector. Because of the high kinetic energy, the excited fragments are expected to leave neon clusters rapidly and emit in the free state. The energy relaxation within the H_2O molecule occurs through high-lying excited electronic states down to repulsive $\tilde{B}(OH^*(A)+H)$ electronic states. If the relaxation involves the lowest bound $\tilde{C}$ state, which rapidly (∼2.5 ps) predissociate into the $\tilde{B}$ state, is not clear. This question could be answered by observing the transient visible $\tilde{C} \rightarrow \tilde{A}$ emission of water molecules [24]. Unfortunately, its intensity is too weak to be observed with SR excitation. Generally, a two-photon powerful laser excitation (∼1 GW/cm^2) is used to detect this emission [24–26].

The probability of the cluster doping was relatively low in our current experiments to avoid multiple doping. The doping efficiency has been estimated by following the intensity of the 70-nm excitation band with increasing the water cross-jet pressure (Fig. 1). The intensity was found to be proportional to the pressure at least below 2.0 mbar, which indicates that the multiple doping is the unlikely process. On the other hand, since the cluster doping is of low probability in these conditions, free water molecules, which are present in the excitation region, may be responsible for a considerable fraction of the fluorescence signal. Therefore, in order to select the fluorescence signal due to dopant only water molecules, we have excited the molecule by the energy transfer process from the excited cluster atoms. The fluorescence of excited fragments was analyzed upon Ne cluster excitation into the lowest excitonic band at 17.7 eV (70.06 nm).

The fluorescence of water vapor in the VUV spectral region has been analyzed in reference [3]. Above the ionization energy of ∼12.6 eV the yield of $OH^*(A)$ is strongly decreased and another higher lying excites states such as $OH^*(B)$ (≥13.6 eV) and $OH^*(C)$ (≥16.0 eV) appear in the reaction exit channel. It was shown that free water molecules excited at 17.70 eV (∼70 nm) result mainly in the following excited dissociation fragments:

$$H_2O + h\nu \xrightarrow{70\ \text{nm}} H_2O^{+*};\ H^*(ns);\ OH^*(C).$$

Among them, $OH^*(C)$ emits in the vacuum ultraviolet. The Balmer $H^*(ns)$-series and the H_2O^{+*} continuum span over the UV-visible spectral region. Low-resolution fluorescence spectra ($\Delta\lambda \approx 6$ nm) of free water molecules and $H_2O@Ne_N$ clusters in the UV-visible are presented in Figure 3. As we have previously observed in H_2O-doped He-clusters [15], the photodissociation channels are not affected by the cluster environment. In Ne clusters the situation is somewhat different. Both, the H-Balmer α-line (H_α) and the H_2O^{+*} continuum observed in case of free H_2O molecules (Fig. 3a) disappear in $H_2O@Ne_N$ clusters and simultaneously the $OH^*(A{-}X)$ emission appears (the emission band at 630 nm is the second order of the principal band at 315 nm). This is shown in Figure 3b. Apparently, the neon cluster strongly affects the reaction dynamics. This cannot be explained by the energy relaxation process within the neon clusters forming m-STE centers followed by the energy transfer to the water molecule. Indeed, the energy transfer to the impurity is generally much more efficient than the matrix relaxation. Moreover, because of the binding energy of ∼0.5 eV and the repulsive ground-state potential between rare-gas atoms,

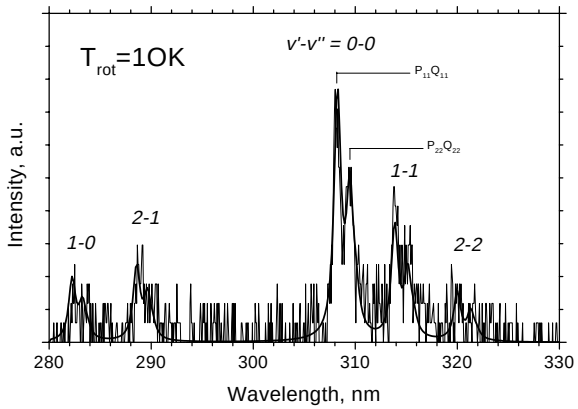

Fig. 4. High resolution $OH^*(A \rightarrow X)$ UV-visible fluorescence spectrum with excitation of $H_2O@Ne_N$ clusters at 70.05 nm. The calculated spectrum with rotational temperature of 10 K is shown by the solid curve.

the m-STE center disposes sufficient electronic energy (∼17–16 eV) to excite H_2O^{+*} (the threshold energy is 13.8 eV). We believe that a new energy relaxation mechanism involved is based on the reaction trajectory perturbation by the cluster environment, which results in the fact that the minor $OH^*(A)$-dissociation channel in free molecules becomes dominant in Ne clusters.

More information on the water photodissociation dynamics in clusters is obtained from high-resolution fluorescence spectra of the $OH^*(A \rightarrow X)$ emission. An example is shown in Figure 4. The relation between the individual rovibronic level population and the fluorescence intensity of the corresponding spectral line is not trivial. As it has been shown in experimental [27] and theoretical [28] studies, the level lifetime can be strongly affected by the predissociation process. For example, the lifetime of the $v' = 0, 1$ vibrational levels ($J' = 0$) is equal to the radiative lifetime of $\tau \sim \tau_{\rm rad} \sim 800$ ns, but it decreases for higher levels as $\tau \sim 130$ ns ($v' = 2$), ∼200 ps ($v' = 3$) and 20 ps ($v' = 4$). As a consequence of this, the luminescence yield q for equal level populations decreases from $q = \tau/\tau_{\rm rad} \approx 1$ ($v' = 0, 1$) to 0.16 ($v' = 2$) and <0.1% for higher levels. The effect of the lifetime shortening also appears in the manifold of the rotational levels and explains, in particular, a strong decrease of the line intensities with $J' > 25$ ($v' = 0$) and with ($J' > 15$) ($v' = 1$). In the following we used the program *LIFBASE* [29] (which account for this effect) to fit the measured high-resolution fluorescence spectra.

It is known from gas phase experiments that $OH^*(A)$ fragments leave with a high amount of rotational and low vibrational excitation [30–32]. This is not the case of the embedded H_2O molecule, where considerable vibrational excitation is found (transitions from $v' = 0, 1, 2$ are clearly observable in the figure): the distribution function appears to be highly inverted with relative populations of the corresponding levels p_0:p_1:p_2 = 0.2:0.2:0.6 (these values have been obtained from the line intensities taking into account the predissociation efficiency factor of $\tau(v')/\tau_{\rm rad}$ discussed above). This result is different from what is expected from theory for free molecules. *Ab initio* calculations performed by Heumann *et al.* [33] predicted that the vibrational excitation of $OH^*(A^2\Sigma)$ fragments is generally weak. Simultaneously, as it follows from our experiments, the rotational excitation of $OH^*(A^2\Sigma)$ is very small. Indeed, the best fitting using the *LIFBASE* program corresponds to a rotational temperature of $T_{\rm rot} \leq 10$ K, which is shown in Figure 4 by a solid line (the calculated spectra, taking into account the experimental spectral resolution, were not sensitive to the rotational temperature below 10 K). At this temperature only lowest rotational levels of the excited vibronic state are populated: R_{11} and R_{22} branches vanish and only heads of series of the Q_{11}, Q_{22}, and P_{11}, P_{22} branches appear as a doublet-like structure (R_{ii}/Q_{ii}) in the spectra [34]. The obtained value of $T_{\rm rot}$ is in excellent agreement with the characteristic temperature of Ne clusters $T_{\rm C} = 10 \pm 4$ K earlier reported by Farges *et al.* [35].

Our results show a strong influence of the cluster environment on the reactivity of the embedded molecule. Apparently, water molecules dope bulk sites of the neon clusters. Following the cluster photoexcitation, energy transfer to H_2O and its dissociation, the $OH^*(A)$ fragment is rotationally thermalyzed inside large Ne_N clusters of a mean size $N \approx 7\,500$. Because the neon matrix induces only a very small line shift [36], we could not conclude from our spectral measurements whether the exited fragments emit from inside of neon clusters or being free. On the other hand, the initial kinetic energy of $OH^*(A)$ after predissociation is high and it likely desorbs from the cluster on a timescale much shorter than its radiative lifetime of ∼800 ns. The difference in relaxation rates between rotational and vibrational levels originates from the coupling efficiency of the doped molecule to the cluster matrix. The molecular constants of $OH^*(A^2\Sigma)$ are $\omega'_{\rm e} \approx 0.36$ eV and $B'_{\rm e} \approx 2.5$ meV and the matrix phonon energy (Debye energy) is $\omega'_{\rm ph} \approx 6.4$ meV. As a result of $B'_{\rm e} \sim \omega_{\rm ph} \ll \omega'_{\rm e}$, the vibrational relaxation proceeds on a longer timescale compared to the rotational relaxation and we suppose that it is not completed during the short residence time of the OH^* fragment inside the Ne cluster. Earlier, Brus and Bondybey [36] have studied the energy relaxation mechanisms of $OH^*(A)$ in the neon matrix *via* time and energy resolved fluorescence. They have found that this molecule behaves almost as a free rotator and the vibrational relaxation is slow indeed ($\sim 10^5$ s^{-1}). Fluorescence lifetime measurements of the selected 2–1 and 1–10 vibronic transitions (on the 10-μs timescale) would be interesting to carry out in $H_2O@Ne_{7500}$ cluster beams to clear up the energy relaxation kinetics related to the spatial position of the emitted $OH^*(A)$ fragments.

The excited-state desorption in clusters can be understood in the framework of the cavity ejection mechanism recently discussed by Laarmann *et al.* [37] in application to the desorption process of $Ar^*(4p)$ atoms in Ar_mNe_N clusters ($m \ll N$). The balance between desorption and solvation depends on the sign and the value of the cluster electron affinity, as it has been earlier proposed for pure and doped rare-gas solids [38,39]. A repulsive interaction between the excited molecule and the cluster atoms

leading to desorption is expected for the negative electron affinity. The experimental results by Laarmann *et al.* [37] show that neon forms a rather soft clusters, which are unable to suppress desorption and to cage excited argon atoms. This seems to be also the case of the excited hydroxide radical.

Moreover, we have observed no caging of neutral hydrogen atoms in neon clusters (which is expected to manifest as the cage-induced quenching of the $OH^*(A)$ fluorescence following the pathway $OH^* + H \xleftarrow{Ar-atoms} H_2O^* \xrightarrow{coupling} H_2O\ (\tilde{X})$ [16]). This result seems to be in some disagreement with reference [11], where the cage effect for photodissociation of the H_2O molecules into neutral ground-state products $H_2O(\tilde{A}) \rightarrow OH(X) + H(1s)$ has been found in solid neon. This difference may be due to the higher-energy excitation of the water molecule in our case as well as the non-crystalline character of the cluster structure. This peculiarity is discussed in the separate paper [16].

3.2 $H_2O@Ar_N$-clusters

Fluorescence of $OH^*(A \rightarrow X)$ dissociation fragments has been observed upon excitation of doped $H_2O@Ar_N$ clusters ($N \approx 400$) in the first excitonic absorption bands of argon clusters at 12 ± 0.4 eV. The energy transfer from the cluster atoms to the water molecule leads to neutral OH^* dissociation fragments. This result is *a priori* expected, since the excitation energy is below the ionization potential of water (12.6 eV). The band intensity increases with the water cross-jet pressure in agreement with what we have observed in $H_2O@Ne_N$ clusters. No UV-visible-IR fluorescence is observed if the water cross-jet is switched off. UV-visible-IR excitation spectra for different Ar_N cluster sizes and a constant water stagnation pressure are presented in Figure 5. In small clusters $N \leq 20$ the excitation spectra are dominated by the $1s$ and $1s'$ (spin-orbit split) surface excitons located at 11.7 eV (106 nm) and 11.9 eV (104 nm), respectively. In larger clusters intense peaks of bulk excitons appear. Simultaneously, the surface excitons do not disappear. The comparison of the UV-visible-IR excitation spectra with the VUV excitation spectra as a function of the cluster size (up to $N \approx 10^3$) has shown that although those intensities are different, the shapes are almost identical. Recent experiments performed by Laarmann *et al.* [37] have shown that the neon surface excitons are absent in visible-IR excitation spectra of Ar_mNe_N clusters ($m \ll N$). This has been interpreted as a perfect solvation of Ar_m clusters in the interior of Ne_N clusters, since no energy transfer to the embedded Ar cluster is observed upon surface excitation. Such surface exciton bands are intense in the fluorescence excitation spectra of our $H_2O@Ar_N$ clusters in Figure 5. Apparently, these observations indicate that the geometric position of the H_2O molecule being on the cluster surface of large Ar clusters is of high probability. In the following we examine fluorescence spectra, which give more arguments for the preferential surface position of the doped water molecule on argon clusters in the crossbeam experiments.

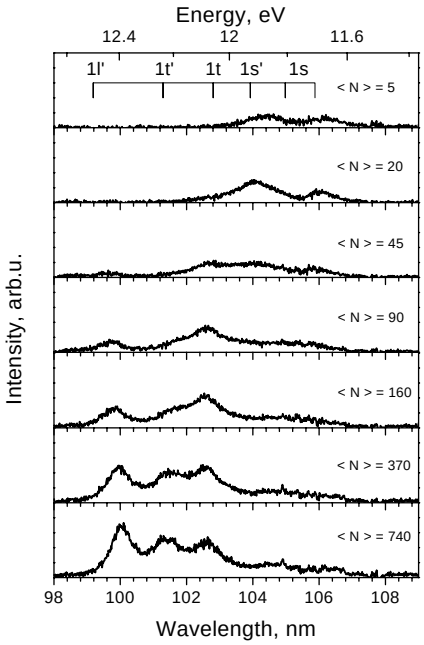

Fig. 5. UV-visible-IR excitation spectra of $H_2O@Ar_N$ clusters for different mean cluster sizes $\langle N \rangle$ with constant water cross-jet pressure $p[H_2O]$= *const*. Vertical lines indicate the excitons of solid argon.

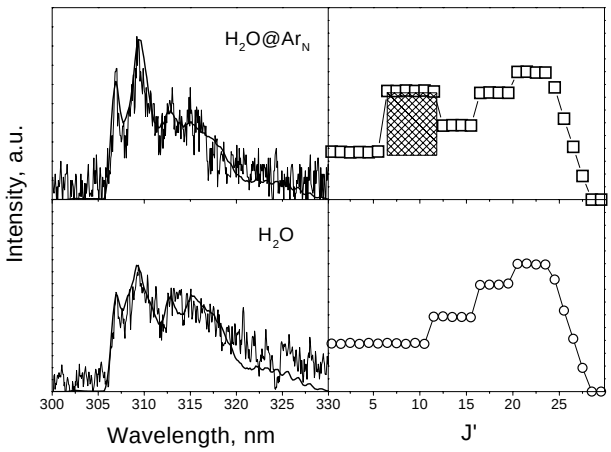

Fig. 6. $OH^*(A \rightarrow X)$ fluorescence spectra (left column) and the rotational distribution function (right column) of free H_2O molecules (lower row) and of doped $H_2O@Ar_N$ clusters (upper row). The best fit spectra are shown by bold solid curves.

More information on the energy transfer process can be obtained from energy resolved fluorescence spectra of $OH^*(A \rightarrow X)$ fragments in the UV spectral region. Two of such spectra, with a direct optical excitation of free water molecules at 102.8 nm from [40] and with the energy transfer from the Ar clusters excited at 102.8 nm, are shown in Figure 6 (left column). The experiments on free water molecules [40] have been carried out in a static cell at water vapor pressures $\sim 10^2$ times higher than used in the present work. It is important to note that because of

the very low concentration of water molecules in the interaction zone with the synchrotron radiation, the direct absorption of photons by water molecules in the cluster beam experiment was negligible: if the cluster beam was switched off, no fluorescence was recorded.

The emission band of $OH^*(A \rightarrow X)$ in solid argon is located at ∼340 nm [11]. In our current experiments no spectral shift due to the interaction with the cluster matrix was observed in the fluorescence spectra. This assures that we observe free $OH^*(A)$ fragments. The shape of the two spectra presented in Figure 6 are somewhat different: a narrow structure which corresponds to transitions from low lying rotational levels (in the band $v' = 0 \rightarrow v'' = 0$) is more intense in doped $H_2O@Ne_N$ clusters compared with free molecules. Simultaneously, the total widths of both spectra are similar. We conclude that the appearance of this specific population of relatively cold $OH^*(A)$ molecules is due to the interaction with the clusters.

To understand the influence of the cluster environment, we have simulated the $OH^*(A-X)$ spectra using the *LIFBASE* program [29]. The experimental spectra are dominated by the $v'-v'' = 0-0$ vibronic transition (80%). The rotational level distributions obtained from the comparison of experimental with calculated spectra are shown in Figure 6 (right column). This is in agreement with previous publications [30–32]. The excited electronic state $A^2\Sigma^+$ of OH fragment ($\Lambda = 0$, $S = 1/2$) belongs to the Hund case b, which characterizes a weak electronic spin coupling with the molecular axis. The total moment is the sum of the nuclei rotation moment ($\mathbf{N}$) and the spin ($\mathbf{S}$): $\mathbf{J}=\mathbf{N}+\mathbf{S}$, and its projection on the axis $J = N \pm 1/2$ is not integer. As it is already known, the predissociation of free water molecules (excited below the ionization limit) releases excited $OH^*(A)$ fragments with a low vibrational excitation and a highly inverted rotational population, which has a maximum near the highest J'-level energetically accessible: $J'_1 = 22.5 \pm 2$. Simultaneously, low rotational levels $J' \leq 10.5$ are poorly occupied. Unfortunately, no analysis of the $OH^*(A)$ spectra with excitation in the spectral range of our interest (∼11.7–12.6 eV) exists in the literature. Following the general tendency, we have used a simple step-like distribution $p_1(J')$ presented in Figure 6 (lower row, right column), which satisfactory reproduces the measured spectrum shown in Figure 6 (lower row, left column). The cluster environment modifies this behavior. We have found that a new population $p_2(J')$ of the $OH^*(A)$ molecule, which desorbs from the cluster, can be presented as a small perturbation of the that earlier obtained $p_1(J')$: $p_2(J') = p_1(J') + p'(J')$. The population $p_2(J')$ has therefore a bimodal character: the second maximum of $p'(J')$ appears at low $J'_2 \approx 8.5 \pm 2$. This is shown in Figure 6 (upper row, right column). A good agreement with the measured spectrum has been obtained in this case. This fraction p' of relatively cold molecules (marked by a filled area in Fig. 6) is still much warmer than the Ar_n clusters, which have a temperature of roughly ∼37 K according to reference [35]. This result in doped argon clusters is completely different from what we have observed in neon clusters, where the complete rotational thermalization of the $OH^*(A)$ fragment in the cluster interior takes place. We believe that the solvated water molecule preferentially takes a surface site of the argon cluster: this results in a slower cooling of the predissociated fragment $OH^*(A)$.

To verify this hypothesis, we have performed calculations using a simple model of the $OH^*(A)$ detachment from the Ar cluster surface. We suppose that this detachment is accelerated by the energy transfer from the rotation into the translational center-of-mass motion. The fragment cooling terminates when it moves from the cluster by the length of the O–H equilibrium distance: in this geometry no more interaction between the fragment and the cluster is possible. OH is considered as a rigid rotator with a reduced mass of $\mu^{-1} = m_{\mathrm{H}}^{-1} + m_{\mathrm{O}}^{-1}$ and a length $l = r_{\mathrm{O-H}}(\mu/m_{\mathrm{H}})$. We assume that because of a small mass of the H atom (m_{H}) the collisional time is short and only one atom (m_{Ar}) of the Ar_n cluster is involved in the collision. Moreover, the kinetic energy of the cluster atom is negligible in the total energy balance of the rigid rotor and we consider it immobile before each collision. This approximation can be justified by the experimental fact that even after the detachment the rotational temperature of $OH^*(A)$ in much higher than the characteristic temperature of the Ar_n clusters (∼37 K). Under these assumptions, the angular velocity (ω) and the velocity of the center-of-mass motion (V) of the fragment before (i) and after (f) collision with the surface Ar atom are expressed as

$$\omega_{\mathrm{f}} = \omega_{\mathrm{i}} \frac{1-\gamma}{1+\gamma} - V_{x\mathrm{i}} \frac{2\sin(\varphi)}{l(1+\gamma)}$$

$$V_{x\mathrm{f}} = V_{x\mathrm{i}} + \frac{m_{\mathrm{Ar}}}{m_{\mathrm{OH}}} \nu \sin(\varphi)$$

where $\gamma = \mu(m_{\mathrm{Ar}}^{-1} + m_{\mathrm{OH}}^{-1})$, $v = l(\omega_1 + \omega_2)\mu/m_{\mathrm{Ar}}$ is the velocity of the Ar atom after collision, φ is the angle between the normal to the cluster surface (x-axis) and the OH molecular axis, and V_x is the x-component of the velocity V. Our numerical calculations show that the $OH^*(A)$ fragment with its initial position in the cluster surface layer may loose $\gamma \approx 80$–90% of its rotational energy leaving the argon cluster. The population of the cooled fraction of the $OH^*(A)$ fragments in the cluster-beam experiment can therefore be obtained from the population measured in a water vapor by simply scaling along the J'-axis: the scaling factor is $(1-\gamma)^{1/2} \approx 0.4$. This is in agreement with the experiment, where the ratio $J'_2/J'_1 \approx 0.4$ has been found. The fraction of cold molecules in p_2 presents only a relatively small contribution ($p' \sim 14\%$) of the total population (filled area in Fig. 6). This means that the reaction channel mainly results in OH^* fragments, which do not have enough time exchanging rotational energy with the cluster surface. This short time may be related to both the initial orientation of OH^* to the cluster surface after the predissociation and to the substantial initial kinetic energy of the center-of-mass motion of the fragment. Our experimental results and the modeling indicate that the preferential position of the trapped water molecule is

on the surface of the Ar_N cluster under standard pick-up conditions.

Theoretical calculations by Lui *et al.* [41] performed on Ar_nH_2O cluster equilibrium structures (n = 1–14) have shown a preference of the solvated geometry: a global minimum of energy for isomers corresponds to a water molecule in the center surrounded by a shell of argon atoms. This seems to be in disagreement with present observations. However, the Ar_N cluster is stable and simply putting a water molecule on the cluster surface may not be sufficient to reorganize its structure: a sufficiently strong annealing is needed for that. In fact, the interaction energy E(Ar–H_2O)≈ 142.9 cm^{-1} is only slightly higher than that of E(Ar–Ar)≈ 99.2 cm^{-1}. In solid argon the binding energy of the argon atoms increases up to 716.2 cm^{-1} because of the high coordination number. This may create a potential barrier prohibiting the guest molecule solvation. The solvation dynamics would be interesting to consider.

Finally, no cage effect has been observed in our Ar_N/H_2O pick-up experiments. The surface position of the water molecule in argon clusters may be a reason, why the cluster does not capture the predissociation products. In a separate paper [16] we present a sequential pick-up technique that allows us to prepare Ar clusters doped with H_2O molecules in interior sites.

4 Conclusion

We have studied the fluorescence of electronically excited dissociation fragments after VUV excitation of rare-gas clusters (Rg = Ne, Ar) doped with H_2O molecules. While H_2O is embedded in the interior of Ne clusters, only surface sites are populated in Ar clusters. The predissociation of a free water molecule above the ionization limit (∼12.6 eV) results in the excited neutral fragments $OH^*(B, C)$ and $H^*(n \geq 2)$ and ions H_2O^{+*}, which emit in the UV-visible spectral region. In contrast to the free water molecule, the $OH^*(A)$ fragment appears to be the main dissociation product in the Ne cluster beam experiments (17.70 eV excitation). The ionic H_2O^{+*} channel is completely suppressed in neon clusters (the effect of the ionic channel suppression has also been earlier reported in He clusters doped with H_2O molecules [15]). The $OH^*(A \rightarrow X)$ emission band has been analyzed in both Ne and Ar cluster (12.06 eV excitation) experiments. The numerical treatment of the experimental spectra shows a bimodal rotational distribution of the reaction exit fragment $OH^*(A)$, which has been explained by the surface position of the impurity molecule in the Ar cluster. The surface doping explains also the fact that we have not observed the cage effect (cage-induced quenching of the excited fragment $OH^*(A) + H \rightarrow H_2O@Ar_N$) in clusters prepared in standard pick-up experiments.

We thank Dr. C. Mc Ginley (HASYLAB) for very helpful discussions. We are grateful to Dr. J.H. Fillion and Professor J.L. Lemaire for permission to reproduce UV fluorescence spectra of vapor H_2O prior to publication. This work was supported by the IHP-Contract HPRI-CT-1999-00040 of the European Commission.

References

1. C.Y.R. Wu, D.L. Judge, J. Chem. Phys. **75**, 172 (1981)
2. G.H.F. Diercksen, W.P. Kraemer, T.N. Rescingo, C.F. Bender, B.V. McLoy, S.R. Langhoff, P.W. Langhoff, J. Chem. Phys. **76**, 1043 (1982)
3. O. Dutuit, A. Tabche-Fouhaile, I. Nenner, H. Frohlich, P.M. Guyon, J. Chem. Phys. **83**, 584 (1985)
4. L.C. Lee, M. Suto, Chem. Phys. **110**, 161 (1986)
5. A. Hodgson, J.P. Simons, M.N.R. Ashfold, J.M. Bayley, R.N. Dixon, Mol. Phys. **54**, 351 (1985)
6. T. Carrington, J. Chem. Phys. **41**, 2012 (1964)
7. L.C. Lee, L. Oren, E. Phillips, D.L. Judge, J. Phys. B: At. Mol. Phys. **11**, 47 (1978)
8. A.H. Zanganeh, J.H. Fillion, J. Ruiz, M. Castillejo, J.L. Lemaire, N. Shafizadeh, F. Rostas, J. Chem. Phys. **112**, 5660 (2000)
9. R. Schriever, M. Chergui, H. Kunz, V. Stepanenko, N. Schwentner, J. Chem. Phys. **91**, 4128 (1989)
10. E.I. Tarasova, A.M. Ratner, V.M. Stepanenko, I.Ya. Fugol, M. Chergui, R. Schriever, N. Schwentner, J. Chem. Phys. **98**, 7786 (1993)
11. B.-M. Cheng, W.-J. Lo, L.-H. Lai, W.-C. Hung, Y.-P. Lee, J. Chem. Phys. **103** 6303 (1995)
12. See relevant articles in issues: Farad. Discuss. **108** (1997), *Dynamics of Electronically Excited States in Gaseous, Cluster and Condensed Media*; Farad. Discuss. **118** (2001), *Cluster Dynamics*
13. L. Moussavizadeh, K. von Haeften, L. Museur, A.V. Kanaev, M.C. Castex, R. von Pietrowski, T. Möller, Chem. Phys. Lett. **305** 327 (1999)
14. L. Museur, A.V. Kanaev, M.C. Castex, L. Moussavizadeh, R. von Pietrowski, T. Möller, Eur. Phys. J. D **7**, 73 (1999)
15. A. Kanaev, L. Museur, T. Laarmann, S. Monticone, M.C. Castex, K. von Haeften, T. Möller, J. Chem. Phys. **115**, 10248 (2001)
16. A.V. Kanaev, L. Museur, T. Laarmann, T. Möller, *Cage effect for photodissociation of H_2O molecule in neon-argon clusters*, HASYLAB Annual Report 2000 (Synchrotron DESY, Hamburg); J. Chem. Phys. (submitted, 2002).
17. R. Karnbach, M. Joppien, J. Stapelfeldt, J. Wörmer, T. Möller, Rev. Sci. Instrum. **64**, 2838 (1993)
18. O.F. Hagena, Surf. Sci. **106**, 101 (1981)
19. O.F. Hagena, Z. Phys. D **4**, 291 (1987)
20. U. Buck, R. Krohne, J. Chem. Phys. **105**, 5408 (1996)
21. R. Karnbach, M. Joppien, T. Möller, J. Chim. Phys. **92**, 499 (1995); R. Karnbach, Ph.D. thesis, HASYLAB DESY, Hamburg, 1993
22. N. Schwentner, E.E. Koch, J. Jortner, *Electronic excitations in condensed rare gases*, Springer Tracts in Modern Physics (Springer, 1985), Vol. 107
23. T. Möller, A.R.B. DeCastro, K. von Haeften, A. Kolmakov, T. Laarmann, J.O. Löfken, C. Nowak, F. Picucci, M. Riedler, C. Rienecker, A. Wark, M. Wolf, J. Elec. Spec. Rel. Phen. **101**, 185 (1999)
24. V. Engel, G. Maijer, A. Bath, P. Andersen, R. Schinke, J. Chem. Phys. **87**, 4310 (1987)
25. G. Meijer, J.J. ter Meulen, P. Andresen, A. Bath, J. Chem. Phys. **85**, 6914 (1986)
26. F. Edery, A. Kanaev, Eur. Phys. J. D (submitted, 2002)
27. J. Brzozowski, P. Erman, M. Lyyra, Phys. Scripta **17**, 507 (1978)
28. D.R. Yarkony, J. Chem. Phys. **97**, 1838 (1992)

29. J. Luque, *LIFBASE* v.1.61, SRI International (March, 1999)
30. T. Carrington, J. Chem. Phys. **41**, 2012 (1964)
31. L.C. Lee, L. Oren, E. Phillips, D.L. Judge. J. Phys. B: At. Mol. Phys. **11**, 47 (1978)
32. A.H. Zanganeh, J.H. Fillion, J. Ruiz, M. Castillejo, J.L. Lemaire, N. Shafizadeh, F. Rostas, J. Chem. Phys. **112**, 5660 (2000)
33. B. Heumann, K. Kühl, K. Weide, R. Düren, B. Hess, U. Meier, S.D. Peyerimhoff, R. Schinke, Chem. Phys. Lett. **166**, 385 (1990)
34. Fine structure of the $^2\Sigma \rightarrow {}^2\Pi$ transitions is discussed in: G. Herzberg, *Molecular Spectra and Molecular Structure, I. Spectra of Diatomic Molecules* (D. van Nostrand Company, Inc., 1966)
35. J. Farges, M.F. De Feraudy, B. Raoult, G. Torchet, Surf. Sci. **106**, 95 (1981)
36. L.E. Brus, V.E. Bondybey, J. Chem. Phys. **63**, 786 (1975)
37. T. Laarmann, K. von Haeften, H. Wabnitz, T. Möller, Surf. Rev. Lett. (2001, in press)
38. M. Runne, G. Zimmerer, Nucl. Instrum. Meth. B **101**, 156 (1995)
39. M. Runne, J. Becker, W. Laasch, D. Varding, G. Zimmerer, M. Liu, R. E. Johnson, Nucl. Instrum. Meth. B **82**, 301 (1993)
40. J.H. Fillion, private communication
41. S. Lui, Z. Bačić, J.W. Moskowitz, J. Chem. Phys. **101**, 8310 (1994)